Geomechanics and Engineering, *Vol. 6*, *No. 1* (*2014*) *17-31*
DOI: http://dx.doi.org/10.12989/gae.2014.6.1.017

Characteristics of failure surfaces induced by embankments on soft ground

Eun-Soo Hong[1], Ki-Il Song*[2], Yeo-Won Yoon[2] and Jong-Wan Hu[3]

[1] BON E&C Co., Ltd. B-610, Seongnam Woorim Lions Vally 2, 146-8, Jungwon-gu, Seongnam-si, Gyeonggi-do, 462-120, Republic of Korea
[2] Department of Civil Engineering, Inha University, 100 Inha-ro, Nam-gu, Incheon, 402-751, Republic of Korea
[3] Department of Civil and Environmental Engineering, College of Urban Science, University of Incheon, Incheon, 406-840, Republic of Korea; and Head of Center, Incheon Disaster Prevention Research Center, University of Incheon, 406-840, Republic of Korea

(*Received September 21*, *2012*, *Revised July 30*, *2013*, *Accepted August 26*, *2013*)

Abstract. This paper investigates the development of failure surfaces induced by an embankment on soft marine clay deposits and the characteristics of such surfaces through numerical simulations and its comparative study with monitoring results. It is well known that the factor of safety of embankment slopes is closely related to the vertical loading, including the height of the embankment. That is, an increase in the embankment height reduces the factor of safety. However, few studies have examined the relationship between the lateral movement of soft soil beneath the embankment and the factor of safety. In addition, no study has investigated the distribution of the pore pressure coefficient *B* value along the failure surface. This paper conducts a continuum analysis using finite difference methods to characterize the development of failure surfaces during embankment construction on soft marine clay deposits. The results of the continuum analysis for failure surfaces, stress, displacement, and the factor of safety can be used for the management of embankment construction. In failure mechanism, it has been validated that a large shear displacement causes change of stress and pore pressure along the failure surface. In addition, the pore pressure coefficient *B* value decreases along the failure surface as the embankment height increases. This means that the rate of change in stress is higher than that in pore pressure.

Keywords: trial embankment; pore pressure coefficient B; lateral movement; failure surface; continuum analysis

1. Introduction

Because of rapid economic growth and a lack of available land, many infrastructure projects have been constructed on marine clay deposits, including those in coastal regions of Peninsular Malaysia and South Korea. In particular, clay deposits along the western coast of Peninsular

*Corresponding author, Assistant Professor, Ph.D., E-mail: ksong@inha.ac.kr

http://www.techno-press.org/?journal=gae&subpage=7 ISSN: 2005-307X (Print), 2092-6219 (Online)

Malaysia are up to 30 meters thick, and the average lateral extent is approximately 25 km (Indraratna *et al*. 1992). The ground subsidence associated with the consolidation of such marine clay deposits can cause substantial damage to structures and lead to civil infrastructure malfunctions (Smith *et al*. 1992). In particular, embankments are crucial structures during the initial stage of highway construction on soft ground. Low shear strength and high excess pore pressure induced by rapid embankment construction can reduce embankment slope stability in the short term, and in the long term, time-dependent ground deformations induced by the consolidation and creep behavior of soft marine clay deposits can cause differential settlement.

Analytical methods and graphical methods have been widely used for analyzing the stability of embankments on soft ground. Because of recent advances in the computational speed of computers, computer-aided numerical analyses have become increasingly popular and are widely used for analyzing slope stability (Kim and Lee 1997). Not only the limit equilibrium method (LEM) but also continuum analysis methods such as the finite element method (FEM) and the finite difference method (FDM) have been used for numerical analyses of slope stability. However, the LEM is generally confined to obtaining the factor of safety and does not address time-dependent deformations and their effects on the factor of safety, which is crucial for long-term embankment slope stability.

Continuum analysis methods can overcome this limitation of the LEM (Kourdey *et al*. 2001). Such methods can be used to evaluate the stability of embankment slopes and thus can facilitate effective construction management based on quantitative and qualitative results. The continuum analysis can produce development of displacement, stress, and pore pressure during embankment construction. During embankment construction, the factor of safety of embankment slopes can be obtained through a continuum analysis based on the strength reduction technique.

A number of studies have evaluated slope stability by using continuum analysis methods (Matsui and San 1992, Dawson *et al*. 1999, Griffiths and Lane 1999, Hammouri *et al*. 2008) and focused mainly on the validity and applicability of such methods in terms of evaluating slope stability. The strength reduction technique, which is a major tool for calculating the factor of safety in the continuum analysis, has been validated in comparative studies based on the LEM (Cheng *et al*. 2007, Wei *et al*. 2009).

Cheng *et al*. (2007) reports that the factor of safety obtained from a continuum analysis using the strength reduction technique is 10-20% less than that obtained from the LEM. The location of tension cracks, the structure of clay layers, and sudden ground water movements are the major reasons for this difference (Hammouri *et al*. 2008). The constitutive model and the plastic flow rule also contribute to the factor of safety (Zhang *et al*. 2011).

The present paper focuses on the characteristics of failure surfaces induced by embankment on soft ground by using numerical tools (the FDM, and the LEM) to analyze the slope stability of trial embankments on soft marine clay deposits that are normally consolidated. The Mohr-Coulomb model and the modified Cam-Clay model are used to define a better constitutive model for the slope stability analysis. The development of failure surfaces is investigated, and the shape of failure surfaces is compared with that of actual failure surfaces. In addition, the relationship between the factor of safety and the lateral movement of soft soil beneath the embankment is investigated. Quality control and management suggestions for embankments on soft marine clay deposits are proposed based on the correlation between the lateral movement and the factor of safety. The distribution of the pore pressure coefficient B value around the failure surface is obtained. Based on a comprehensive analysis of the failure surface, the failure mechanism induced by embankments on soft marine clay deposits is interpreted through a continuum analysis.

2. Introduction to numerical analysis

2.1 Limit equilibrium method

The LEM, introduced by Fellenius (1936) and Taylor (1937) and extended by many other researchers (e.g., Petterson 1955, Bishop 1955, Morgenstern and Price 1965), analyzes ground stability based on the simple static mechanical theory under simplified boundary conditions along a fictitious failure surface. The LEM takes an iterative approach to identify failure surfaces, which provide the minimum factor of safety based on the force equilibrium between sliced soil masses. In the LEM, active failure surfaces have circular, planer, or noncircular shapes. Fig. 1 shows a schematic diagram of the Bishop method (Bishop 1955). As shown in Eq. (1), the factor of safety can be determined from the ratio of the driving shear force to the resisting shear force along the slip surface

$$F_s = \frac{1}{\sum W \cdot \sin(\alpha)} \sum \left\{ c \cdot b + \left(W \cdot \tan(\varphi) + \Delta T \cdot \tan(\varphi) \right) \right\} \frac{1}{m_a} \tag{1}$$

$$m_a = \cos(\alpha) + \frac{\tan(\varphi) \cdot \sin(\alpha)}{F_s} \tag{2}$$

where W is the weight of the slice, α is the angle, c is cohesion, φ is the internal friction angle, b is the width of the slice, ΔT is the shear force, and F_s is the factor of safety.

In the LEM, fictitious failure surfaces should be defined to calculate the factor of safety. Assumptions about sliced soil masses and equilibrium conditions are slightly different depending on the approach, and different assumptions about interacting forces in slices can produce different results for the factor of safety and the failure surface (Morgenstern and Price 1965, Janbu 1954, Revilla and Castillo 1977, Baker and Garber 1978, Merrien-Soukatchoff and Omraci 2000). The LEM has been widely used for designing slopes based on the factor of safety because it provides a reasonable factor of safety for potential failure surfaces and is simple and robust. Unfortunately, the inherent composition and stress history of a particular area of land cannot be considered in the LEM. In addition, the LEM provides no information on the settlement of the embankment body and changes in the time-dependent factor of safety induced by ground consolidation.

This paper uses Slide (Rocscience 2010) in conjunction with TCON (Taga Engineering 1991) to analyze slope stability. Slide is a widely used program for analyzing slope stability and can consider saturation, discontinuity, tension cracks, and seismic loading. TCON is a 1D Terzaghi consolidation analysis program. The displacement and changes in soil parameters induced by consolidation can be obtained through TCON. Changes in the void ratio, permeability, and the volumetric compression coefficient can be obtained through TCON simulations during the consolidation process. Therefore, the limitation of the LEM can be addressed by employing Slide in conjunction with TCON to analyze the slope stability of embankments on soft marine clay deposits.

2.2 Continuum analysis using the strength reduction technique

The FDM and the FEM represent the most popular continuum analysis techniques. The FDM program used in this paper is FLAC2D (ITASCA 2002). Governing equations include the

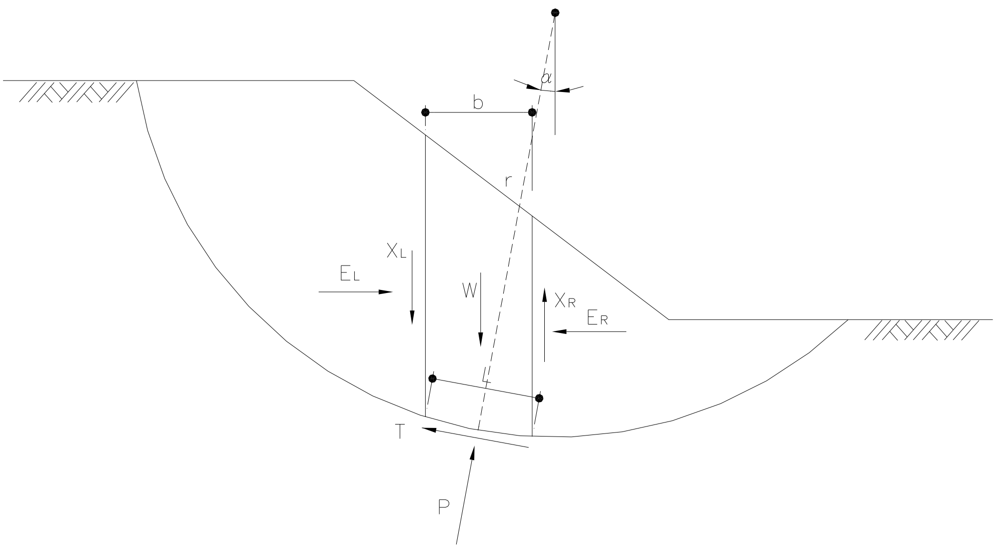

Fig. 1 The forces acting on a slice

equilibrium equation, the compatibility equation, and equations of motion are used to define the discretized 2D domain. An explicit time-marching solution to full equations of motion (including inertial terms) permits an analysis of progressive failures and collapse. The initial and boundary conditions are applied to equations of motion to calculate displacement, stress, and strain. The iterative calculation is carried out through the FDM analysis to determine an equilibrium solution that satisfies the pre-defined unbalance force or the number of steps.

The strength reduction technique, introduced by Zienkiewicz *et al*. (1975) and validated by Griffiths and Lane (1999) and Matsui and San (1992), has been used to calculate the factor of safety in the continuum analysis. Fig. 2 shows the basis of the strength reduction technique. Cohesion and the friction angle at the failure state can be defined as follows

$$c_f = \frac{c}{F_s} \tag{3}$$

$$\varphi_f = \arctan\left(\tan\frac{\varphi}{F_s}\right) \tag{4}$$

where c_f is cohesion at the failure state and φ_f is the internal friction angle at the failure state.

In general, the strength reduction technique is used to calculate the factor of safety by gradually reducing the shear strength of the material. This technique entails a series of simulations using trial values of strength parameters such as cohesion and the friction angle, which are divided by the factor of safety until they reach the critical state. Through a series of automatic simulations with changes in strength parameters, the factor of safety that corresponds to the point of stability is found, and the critical failure surface is determined. Therefore, assumptions about fictitious failure

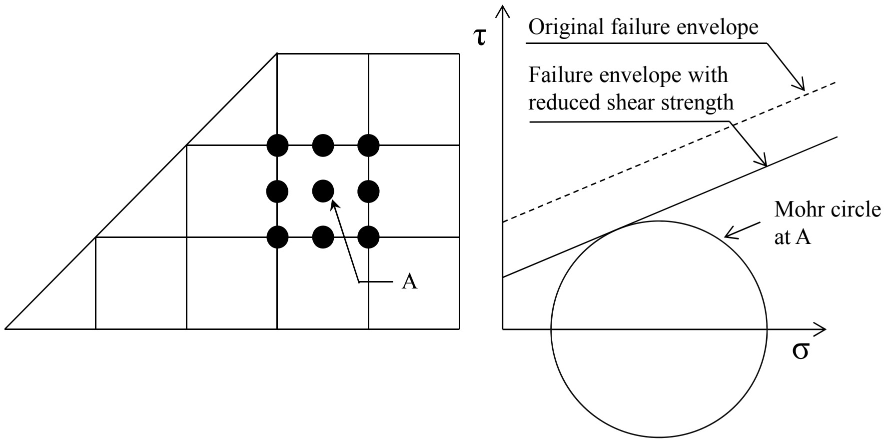

Fig. 2 Strength reduction technique in continuum analysis

surfaces, interacting forces between slices, and their direction are not necessary for calculating the factor of safety by using this technique. In addition, the progressive failures and stress change can be considered during the calculation process. Therefore, the uncertainty associated with the analysis of slope stability can be reduced using the strength reduction technique.

3. Trial embankment and preliminary analysis

3.1 Muar trial embankment

The behavior of marine clay deposits distributed along the western coast of Peninsular Malaysia was examined to find the best stabilization method for the North-South expressway construction. Marine clay deposits in the Muar area are 10-20 meters thick and have high moisture content and low undrained shear strength, which can cause problems during the construction and operation of the expressway. An analysis of the compatibility of various stabilization methods and construction costs was conducted through a trial embankment. Therefore, full-scale trial embankments were constructed in 1986 to investigate the behavior of soft marine clay deposits (Indraratna *et al*. 1992).

Nine types of soft-ground stabilization methods suggested by various construction companies were applied to 13 trial embankments. The area of the trial embankment is 50 m by 50 m. The height of 9 embankments is 6 m, and that of the remaining 4 embankments is 3 m. One trial embankment using no soft-ground stabilization methods was constructed until it reached the failure state. Fig. 3 shows the representative Muar trial embankment.

In this paper, FLAC2D is used to simulate the Muar trial embankment. A failure has been reported at 5.5 m of the embankment. Therefore, the sequential construction process is simulated through seven stages (1 m, 2 m, 3 m, 4 m, 4.5 m, 5 m, and 5.5 m). Material properties of Muar marine clay deposits are taken from research done by Indraratna *et al*. (1992) as summarized in Table 1. A comparative analysis is conducted to investigate the correlation between the lateral

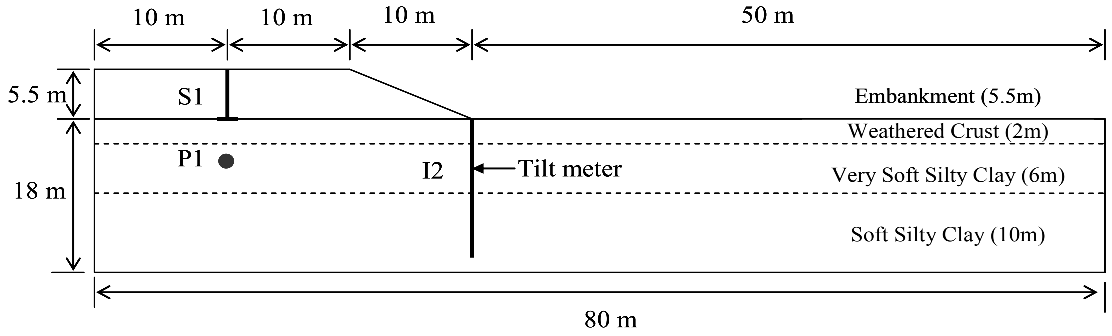

Fig. 3 Sections of Muar trial embankments

movement of soft soil beneath the embankment and the factor of safety of the embankment slope by using the FDM and the LEM. Geotechnical parameters of soft soil vary during the consolidation process. It should be considered in slow construction on soft soil. However, it has been reported that the Muar trial embankment was built at a rate of 0.4 m per week, which is much faster than the amount of time needed for the dissipation of excess pore pressure (e.g., 6,000 days). Therefore, a total stress analysis under the undrained condition is conducted for the Muar trial embankment. Thus, change of geotechnical parameter is not taken into account in present study. The ground water flow into the embankment body is not considered in this paper.

Because the LEM cannot consider the settlement induced by the consolidation process, a consolidation analysis using TCON is conducted, and the results are combined with those of the slope stability analysis. Embankment settlement data obtained using TCON are considered for the analysis of slope stability in successive stages. In addition, original shear strength parameters are used only for the initial stage. For the analysis of slope stability in subsequent stages, shear

Table 1 Material properties for Muar trial embankment

Mohr-Coulomb model	E (kN/m^2)	υ	γ_t (kN/m^3)	c (kN/m^2)	φ (°)	k (m/day)
Muar embankment	5100	0.3	16.5	19	26	8.64
Muar crust	25500	0.3	16.5	15.4	6.5	1.3E-4
Muar very soft silty clay	6600	0.3	15.5	10+2.3ΔZ	13.5	1.3E-4
Muar soft silty clay	5800	0.3	15.5		17	9.5E-05
Modified Cam-Clay model	M	λ	κ	Pc (kPa)	e_{cs}	Ko
Muar crust	1.19	0.13	0.05	110	3.07	0.6
Muar very soft silty clay	1.07	0.13	0.05	40	1.61	0.6
Muar soft silty slay	1.07	0.11	0.08	60	1.55	0.6

*where, E is Elastic modulus, υ is Poisson's ratio, γ_t is unit weight, c is cohesion, φ is friction angle, and k is permeability, respectively. M, λ, κ are Modified Cam-clay model parameters, Pc is pre-consolidation pressure, e_{cs} is critical state void ratio, Ko is lateral earth pressure coefficient at rest.

strength parameters are updated based on the time-dependent consolidation ratio. For the FDM analysis, the dimensions of model are identical to LEM model as shown in Fig. 3. The strength parameters are updated based on the time-dependent consolidation ratio. For the FDM horizontal displacement is fixed at both sides, and the vertical displacement is fixed at the bottom of the analysis model. For the calculation of factor of safety, strength reduction technique which is embedded in FLAC2D is adopted. The unit weight of water is 10 kN/m^3, and the static water pressure distribution is considered. Only half of the embankment is considered because of the symmetry.

3.2 Analysis of constitutive models

The behavior of an embankment depends on the material model in the continuum analysis (FDM). The results obtained using the Mohr-Coulomb and modified Cam-Clay models for the Muar trial embankment are compared with data from field monitoring and the findings of previous

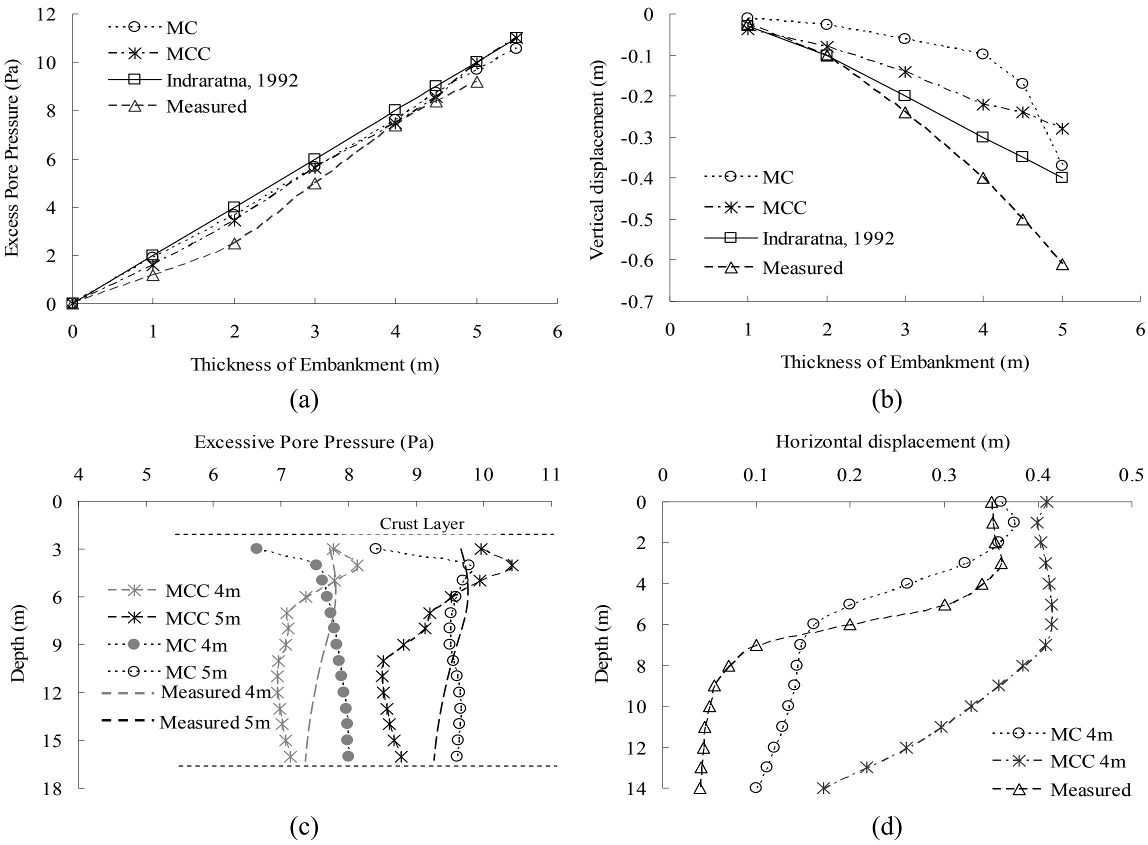

Fig. 4 Mechanical behavior of Muar trial embankment (a) Excess pore pressure at P1 (b) Vertical displacement at S1 (c) Excess pore pressure distribution at the center of embankment (d) Horizontal movement in failure state at I2 (Note: MC denotes Mohr-Coulomb model and MCC denotes Modified Cam-Clay model)

research. Fig. 4(a) shows the development of excess pore pressure according to the height of the embankment at P1 from Fig. 3 (4.5 m from the ground surface). Excess pore pressure obtained from the numerical analysis using the Mohr-Coulomb and modified Cam-Clay models is consistent with the field data, which implies that the undrained condition is valid for the Muar trial embankment simulation.

Fig. 4(b) shows the vertical displacement according to the height of the embankment at S1 from Fig. 3. There is a large difference between the field data and the results of the numerical simulation. This may be largely due to the simplification of the numerical simulation. For example, the simulation does not consider the compaction effect of heavy vehicles during embankment construction. The vertical displacement obtained from the Mohr-Coulomb model is smaller than that obtained from the modified Cam-Clay model.

The distribution of excess pore pressure at the center of the embankment is presented in Fig. 4(c). Excess pore pressure obtained using the Mohr-Coulomb model is consistent with the field data. That is, the predicted excess pore pressure is slightly lower at the top and slightly higher at the bottom. The lateral movement obtained at I2 from Fig. 3 is shown in Fig. 4(d) for the case in which the embankment height is 4 m. The lateral movement obtained from the Mohr-Coulomb model is consistent with the field data.

The overall behavior of the embankment and the development of pore pressure can be simulated using the Modified Cam-Clay model. However, the development of the shear failure surface and the lateral movement of the soft soil beneath the embankment cannot be efficiently modeled using the modified Cam-Clay model. On the other hand, the Mohr-Coulomb model can be effectively used to simulate the shear failure surface and the development of excess pore pressure induced by the embankment construction. In addition, the strength reduction technique can be incorporated with Mohr-Coulomb model to calculate the factor of safety. Therefore, the correlations between the factor of safety, the lateral movement, and excess pore pressure are investigated using the Mohr-Coulomb model for the Muar trial embankment.

4. Continuum and limit-equilibrium analyses

4.1 Factor of safety

As shown in Fig. 5, it is clear that the higher the embankment, the lower the factor of safety. When the height of the embankment exceeds 4 m, the factor of safety obtained from the LEM decreases continuously and becomes lower than that obtained from FDM in the undrained condition. In addition, the factor of safety obtained from the FDM is lower than that obtained from the LEM in the drained condition, which is consistent with the findings of previous studies.

The factor of safety of the embankment slope during construction is influenced by various factors such as increases in body weight, the settlement of the embankment body, increases in effective stress from consolidation, and increases in shear strength. A continuum analysis provides the distribution of stress, the distribution of excess pore pressure, and the deformation of the embankment, which means that deformations, pore pressure, and redistributed stress influence calculations in subsequent stages. However, the LEM analysis cannot consider the aforementioned behavior of the embankment and thus results in a higher factor of safety. Therefore, the LEM needs to be combined with the consolidation analysis in considering the strength of shear parameters and the settlement of the embankment body for a rational calculation of the factor of safety.

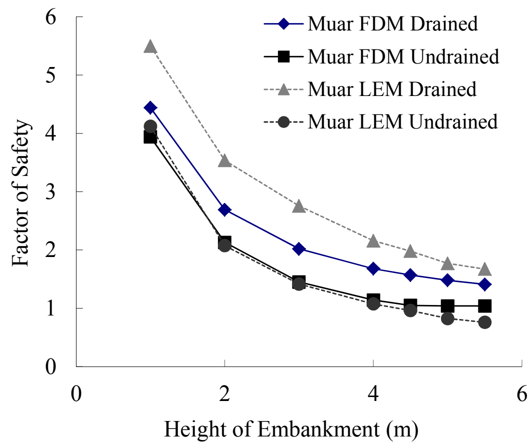

Fig. 5 Effect of height of Muar trial embankment on factor of safety

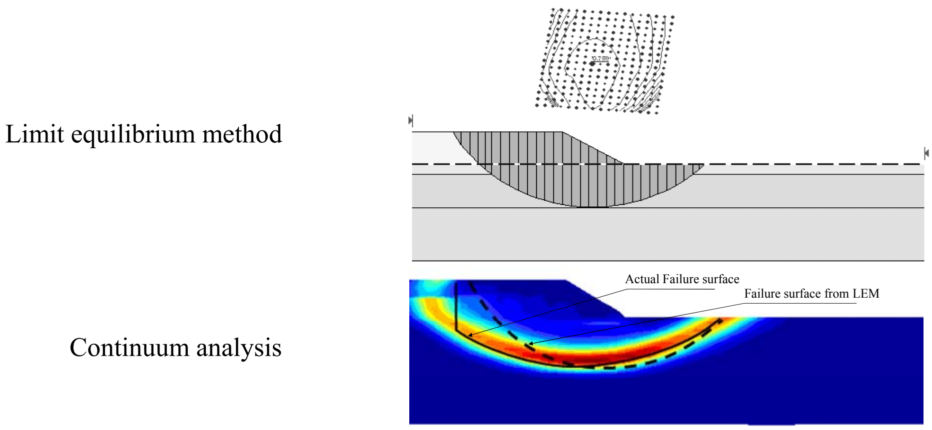

Fig. 6 Effect of height of Muar trial embankment on factor of safety

4.2 Development of the failure surface

The factor of safety and the development of the failure surface and its shape are the most important issues in the slope stability of embankments. Because of embankment loading, a large accumulation of shear stress can cause tension cracks at the top of the embankment, and excess pore pressure, which reduces effective stress, can develop in marine clay deposits (which are not very permeable). When shear stress exceeds shear strength, the local area reaches a critical state, and the yielded area propagates through weak ground. Finally, active failure surfaces form along the yielded region.

Failure surfaces obtained from the LEM and the continuum analysis for the Muar trial embankment are shown in Fig. 6. According to Hudson *et al.*'s (1989) LEM analysis of the embankment height and the depth of the failure surface for the Muar trial embankment, the embankment height at the failure state ranges from 2.8 m to 9.5 m (average = 4.7 m; standard distribution = 1.5 m; actual height = 5.5 m), and the depth of the failure surface ranges from 2.5 m to 13 m (average = 6.3 m; standard distribution = 2.2 m; actual depth = 8 m). As shown in Fig. 6, the shape and depth of the failure surface obtained using the LEM are not consistent with those of the actual failure surface. However, the failure surface with tension cracks obtained using the FDM is consistent with the actual failure surface of the Muar trial embankment.

Predefined failure surfaces should be assumed to produce a minimum factor of safety in the LEM analysis. Therefore, failure surfaces obtained using the LEM can be different from actual failure surfaces. However, failure surfaces obtained using the strength reduction technique in the continuum analysis are similar to actual failure surface because the critical yield state can be simulated by reducing shear strength, which is a more realistic condition for slope failures.

4.3 Correlation between the horizontal displacement and the factor of safety

The vertical displacement and lateral movement of the ground surface cannot represent the overall behavior and associated slope stability of an embankment because the embankment is influenced by various ground conditions, complicated construction processes, foundation improvements, and the installation of reinforcement structures. However, it has been reported that the lateral movement beneath the embankment is coherently related to its height (Travenas and Bouges 1979). As discussed earlier, the factor of safety of the embankment slope is closely correlated with the embankment height, and therefore the relationship between the lateral movement of soft soil beneath the embankment and the factor of safety can be examined.

The relationships between the height, lateral movement, and factor of safety of the embankment obtained through a continuum analysis for the Muar trial embankments are presented

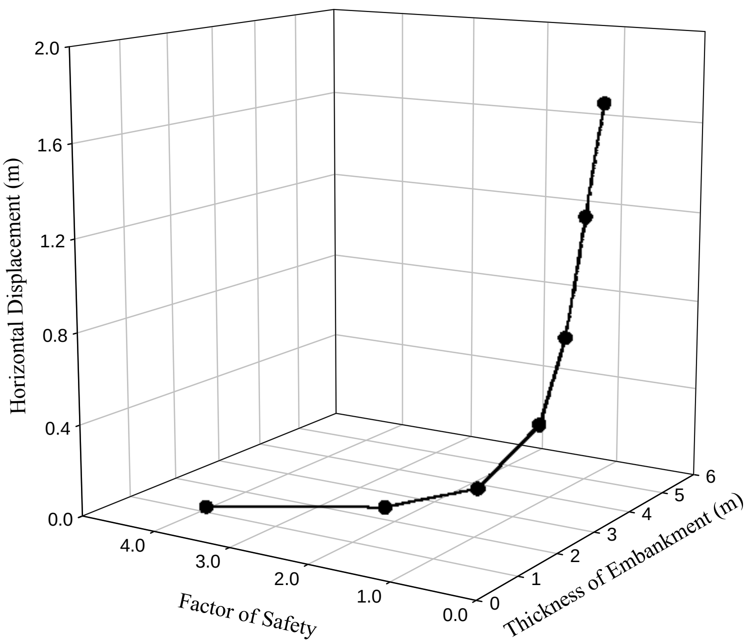

Fig. 7 Inter-relation between height of embankment, factor of safety, and thickness of embankment

in Fig. 7. The maximum lateral movement is obtained at 4 m below the toe of the Muar trial embankment. In general, an increase in the embankment height reduces the factor of safety and increases the lateral movement for both embankments. The lateral movement increases linearly over 4 m of embankment construction, and the factor of safety decreases to 1.15~1.20. Based on Hunter and Fell (2003), the lateral movement, which is closely related to the embankment height, increases sharply at the critical embankment height. Therefore, an impending embankment slope failure can be predicted from a rapid increase in the heave movement rate at the bottom of the toe. Based on an analysis of 13 cases of embankment failures (Hunter and Fell 2003), the critical embankment height showing an impending embankment failure is 70-90 % of the embankment height at the failure state. The results for the Muar trial embankment are consistent with the findings of previous studies. The critical embankment height is 4 m, which is 74 % of the embankment height at the failure state (5.5 m), and the continuum analysis indicates that the factor of safety is 1.2.

In summary, the lateral movement, factor of safety, and height of the embankment are closely correlated. A comprehensive relationship can be obtained through a continuum analysis, and the results can be used to control and manage embankment construction based on the time-dependent consolidation of soft marine clay deposits. Therefore, the factor of safety of the embankment slope can be estimated using field data on the lateral movement at the bottom of the toe. In addition, the speed of embankment construction can be estimated such that it does not exceed the critical factor of safety (1.2).

4.4 Spatial distribution of the pore pressure coefficient B value

The pore pressure coefficient *B* value, the ratio of changes in pore pressure to changes in mean stress (Skempton 1954), varies according to the depth and can be calculated as follows

$$B = \frac{\Delta u}{(\Delta\sigma_{yy} + 2\Delta\sigma_{xx})/3} \tag{5}$$

Excess pore pressure induced by embankment construction transforms the distribution of *B* value. It has been reported that the average value of *B* value in the initial stages of embankment construction is 0.4 (Tavenas and Leroueil 1980). However, the development speed of excess pore pressure induced by staged construction and its magnitude are not consistent with the evolution of shear stress. Therefore, *B* value is spatially distributed.

A FISH program is developed to calculate *B* value by using FLAC2D. Fig. 8 shows the distribution of *B* value when the height of the Muar trial embankment is 5.5 m. Technically, *B* value should be 1.0 beneath the embankment body under the undrained condition when clay deposits are fully saturated with ground water. Because *B* value is a function of excess pore pressure and mean stress, it is influenced by the embankment construction process. The FDM simulation indicates that *B* value is less than 1.0 and spatially distributed. In addition, as shown in Fig. 8, the distribution of *B* value forms a discontinuous line coinciding with the active failure surface.

The level of stress changes as the embankment height. In particular, a high level of shear stress develops, and associated large shear strain increment forms a failure surface. A high level of shear stress is concentrated more along the failure surface than the neighboring ground when the height of the embankment is 5.5 m (Fig. 9). Horizontal stress increases as the height of the embankment increases. However, vertical stress is continuous at the bottom of the embankment body and does not influence the failure surface. Therefore, the horizontal stress increment has a greater effect on *B* value than the vertical stress increment.

Fig. 10 shows the changes in *B* value according to the embankment height. The distribution of *B* value for a 1 m embankment is subtracted from that for a 4.5 m, 5.0 m, or 5.5 m embankment. As the embankment height increases, the distribution of *B* value is increasingly discontinuous at the location of the failure surface where the shear strain increment is large. The shape and size of the discontinuous band of *B* value increases and becomes clearer as the thickness of the embankment increases.

In summary, *B* value decreases along the failure surface as the embankment height increases. This means that the rate of change in stress is higher than that in pore pressure. A large shear displacement can cause high levels of excess pore pressure and shear stress along the failure surface.

Fig. 8 Distribution of pore pressure coefficient *B* at 5.5 m of embankment height

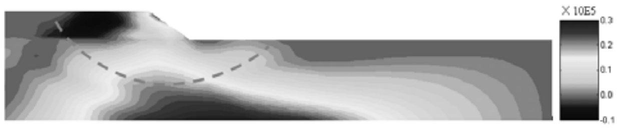

Fig. 9 Shear stress distribution at 5.5 m of embankment height

(a) $B_{4.5}$ - B_1

(b) B_5 - B_1

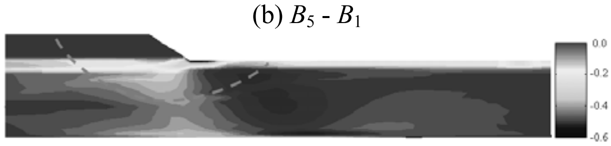

(c) $B_{5.5}$ - B_1

Fig. 10 Development of relative pore pressure coefficient *B* value along the failure surface in Muar trial embankment (a) at 4.5 m of embankment height (b) at 5.0 m of embankment height (c) at 5.5 m of embankment height

5. Conclusions

This paper examines the stability of the embankment slope through an LEM analysis and a continuum analysis using the FDM. The paper considers trial embankment on normally consolidated marine clay deposit in terms of the factor of safety, the lateral movement, the failure surface, and the pore pressure coefficient *B* value.

The strengthening of soil parameters and settlement induced by consolidation is considered through an LEM analysis using the 1D Terzaghi consolidation program. For the factor of safety based on a continuum analysis, the strength reduction technique is used. In addition, a FISH program embedded in FLAC is developed to calculate *B* value at the bottom of the embankment during the construction process.

Although the LEM has been widely used for analyzing slope stability because it provides a relatively reliable factor of safety based on a minimum number of input parameters, an active failure surface providing a minimum factor of safety should be assumed or identified. The factor of safety and the potential failure surface vary according to assumptions about interacting forces and equilibrium states between slices. On the other hand, the continuum analysis provides not only the factor of safety but also the failure surface, the distribution of pore pressure, the time-dependent displacement of the embankment, and the elasto-plastic behavior of soft soil. Therefore, it is possible to obtain the correlations between the factor of safety, the lateral movement, and the embankment height through a continuum analysis. However, for a successful continuum analysis, there needs to be a good understanding of various material models and their parameters, reasonable engineering judgments about dominant conditions such as undrained or drained conditions, and various analysis options such as an analysis of effective stress or total stress based on the speed of embankment construction. The results verify the feasibility of using the continuum analysis to examine the slope stability of embankments.

The development of the shear failure surface and the distribution of *B* value for the failure surface explain the changes in displacement, shear stress, and pore pressure on the failure surface. The decrease in *B* value along the failure surface exceeds that along the neighboring ground, indicating that the rate of change in stress is higher than that in pore pressure.

The lateral movement is closely related to the failure of the embankment slope. Because the discontinuity of *B* value is observed on the failure surface where the shear strain increment is larger than that for the neighboring ground, the failure of the embankment slope cannot be predicted by monitoring excess pore pressure in the field. The results indicate that the lateral movement can be converted into the factor of safety. This suggests that successful quality control and management can be achieved for embankments on soft marine clay deposits by considering the correlation between the lateral movement and the factor of safety obtained through a continuum analysis.

Acknowledgments

This research was supported by Basic Science Research Program through the National Research Foundation of Korea (NRF) funded by the Ministry of Science, ICT & Future Planning (NRF-2013R1A1A1060052). Also, this research was supported by a grant from 2013 Research Development Program at Incheon Green Environment Center.

References

Baker, R. and Garber, M. (1978), “Theoretical analysis of the stability of slopes”, *Geotechnique,* **28**(4), 395-411.
Bishop, A.W. (1955), “The use of the slip circle in the stability analysis of slopes”, *Geotechnique,* **5**(1), 7-17.
Cheng, Y.M., Lansivaara, T. and Wei, W.B. (2007), “Two-dimensional slope stability analysis by limit equilibrium and strength reduction methods”, *Comput. Geotech.,* **34**(3), 137-150.
Dawson, E.M., Roth, W.H. and Drescher, A. (1999), “Slope stability analysis by strength reduction”, *Geotechnique,* **49**(6), 835-840.
Fellenius, W. (1936), “Calculation of the Stability of Earth Dams”, *Proc. of the Second Congress of Large Dams 4*, 445-463.
Griffiths, D.V. and Lane, P.A. (1999), “Slope stability analysis by finite elements”, *Geotechnique*, **49**(3), 387-403.
Hammouri, N.A., Malkawi, A.I.H. and Yamin, M.M.A. (2008), “Stability Analysis of slope using the finite element method and limiting equilibrium approach”, *Bull. Eng. Geol. Env.,* **67**(4), 471-478.
Hudson, R.R., Toh, C.T. and Chan, S.F. (1989), *International Symposium on Trial Embankments on Malaysian Marine Clays*, Kuala Lumpur, November, Vol. 1-3.
Hunter, G. and Fell, R. (2003), “Prediction of impending failure of embankments on soft ground”, *Can. Geotech. J.,* **40**(1), 209-220.
Indraratna, B., Balasubramaniam, A.S. and Balachandran, S. (1992), “Performance of test embankment constructed to failure on soft marine clay”, *ASCE. J. Geotech. Eng.,* **118**(1), 12-33.
ITASCA (2002), FLAC—Fast Lagrangian Analysis of Continua, version 4.0., Minneapolis (MN), Itasca Consulting Group, Inc.
Janbu, N. (1954), “Applications of composite slip surfaces for stability analysis”, *Proceedings of European Conference on the Stability of Earth Slopes*, Stockholm, Sweden, Vol. 3, pp. 43-49.
Kim, J.Y. and Lee, S.R. (1997), “Improved search strategy for critical slip surface in stress fields obtained by finite element method”, *Comput. Geotech.,* **21**(4), 295-313.
Kourdey, A., Alheib, M. and Piguet, J.P. (2001), “Evaluation of slope stability by numerical methods”, *The 17th International Mining Congress and Exhibition of Turkey, IMCET 2001*, Ankara, Turkey, pp. 705-710.
Merrien-Soukatchoff, V. and Omraci, K. (2000), “Détermination des conditions aux limites pour un calcul de stabilité de talus”, *Revue Française de Géotechnique,* **92**, 31-39.
Matsui, T. and San, K.C. (1992), “Finite element slope stability analysis by shear strength reduction technique”, *Soils Found*., **32**(1), 59-70.
Morgenstern, N.R. and Price, V.E. (1965), “The analysis of the stability of general slip surfaces”, *Geotechnique,* **15**(1), 79-93.
Petterson, K.E. (1955), “The early history of circular sliding surfaces”, *Géotechnique,* **5**(4), 275-296.
Revilla, J. and Castillo, E. (1977), “The calculus of variations applied to stability of slopes”, *Geotechnique,* **27**(1), 1-11.
Rocscience Inc. (2010), Analysis and Design Programs for Civil Engineering and mining Applications, www.rocscience.com
Skempton, A.W. (1954), “The pore pressure coefficients A and B”, *Geotechnique,* **4**(4), 143-147.
Smith, P.R., Jardine, R.J. and Hight, D.W. (1992), “The yielding of Bothkennar clay”, *Geotechnique,* **42**(2), 257-274.
Taga Engineering (1991), TCON, Calculation of Consolidation Settlements and Rates of Settlement, TAGA Engineering Software Ltd., www.Tagasoft.com
Tavenas, F. and Leroueil, S. (1980), “The behaviour of embankments on clay foundations”, *Can. Geotech. J.,* **17**(2), 236-260.
Taylor, D.W. (1937), “Stability of earth slopes”, *J. Boston Soc. Civ. Eng.,* **24**, 197-246.
Travenas, F. and Bouges, M.F. (1979), “Lateral displacement in clay foundation under embankments”, *Can.*

Geotech. J., **16**(3), 532-550.
Wei, W.B., Cheng, Y.M. and Li, L. (2009), “Three-dimensional slope failure analysis by the strength reduction and limit equilibrium methods”, *Comput. Geotech.,* **36**(1-2), 70-80.
Zhang, K., Li, W. and Shi, J. (2011), “FEM stability analysis on soil slope with different constitutive models”, *Slope Stability and Earth Retaining Walls (GSP 216), Proceedings of the 2011 GeoHunan International Conference, ASCE*.
Zienkiewicz, O.C., Humpheson, C. and Lewis, R.W. (1975), “Associated and non-associated visco-plasticity and plasticity in soil mechanics”, *Geotechnique*, **25**(4), 671-689.

GC